ECS Transactions, 58 (3) 175-184 (2013)
10.1149/05803.0175ecst ©The Electrochemical Society

The Stability and Ionic Conductivity in Cr Doped $Y_2Ti_2O_7$ in the Search for Potential SOFC Electrolyte Materials

Hao-En Hung, Chia-Kan Hao, and Chi-Shen Lee*

*Department of Applied Chemistry, National Chiao Tung University, 300 Hsinchu, Taiwan
E-mail: *chishen@mail.nctu.edu.tw*, Tel: +886-3-5131332

In this study, a series of $Y_2Ti_{2-x}Cr_xO_7$ were synthesized by sol-gel method and characterized by powder X-ray diffraction (PXRD), scanning electron microscope energy dispersive spectroscopy (SEM-EDS), inductively coupled plasma atomic emission spectroscopy (ICP-AES), temperature-programmed reduction (TPR), and AC-impedance to investigate their properties for the application of intermediate temperature solid oxide fuel cell (IT-SOFC). $Y_2Ti_{2-x}Cr_xO_7$ existed single-phase in a range of $0 < x \leq 0.8$. The refined cell parameters decreased as the amount of doped Cr concentration increased. In addition, the TPR profiles showed that the as-prepared materials started to react with hydrogen in the temperature range of 350 - 450 ºC. The analyzed results of XPS suggested that the average oxidation state of Cr decreased with the increased Cr content. Measurements of ionic conductivities induced that the optimized performance was observed at x = 0.2 with 0.01 S/cm at 700 ºC due to an optimized condition of carrier concentration and carrier mobility. The ionic conductivity dropped under reducing condition, indicative of a p-type semiconductor. The as-prepared $Y_2Ti_{1.8}Cr_{0.2}O_7$ exhibits low electrical conductivity (0.0004 S/cm at 700 ºC) and good ionic conductivity, which is potentially suitable to be utilized as an electrolyte material for IT-SOFC.

Introduction

Solid oxide fuel cell is a promising energy technology that allow for the direct electrochemical conversion of fuel to electricity. The conventional SOFCs operate at high temperature of ~900 ºC and suffer for fast degradation rate of cell and high cost of materials. Therefore, SOFCs that operate at intermediate temperatures between 600 ºC and 700 ºC (IT-SOFCs) have been a focus of many development efforts. The performance of IT-SOFCs is strongly affected by on the electrochemical property of cathode–electrolyte interface, since the interfacial polarization increases rapidly as the temperature is decreased. (1) Potential electrolyte materials for IT-SOFCs should have better ionic conductivity compare to that than YSZ below 700 ºC. Among these materials, pyrochlores with the general formula $A_2B_2O_7$ (usually A^{III}/B^{IV} and A^{II}/B^{V}) are a promising candidate due to their ability for partial replacement of metal ions in A and B sites. They have received attention for their stability at high-temperature and flexible cation combinations that can tailor the structural stability and electrical properties to meet

the requirements for SOFCs. The introduction of aliovalent cation gives rise to oxygen vacancies as charge compensating defects thereby enhancing the ionic conductivity. Moreover, disordering in cations or anions results in-order − disorder transition. The magnitude of this disordering enhances the formation of anion Frankel defects, which leads to good ionic conductivity.

Many pyrochlore phases exhibit high ionic conductivity. For example, $(Ln_{0.9}Ca_{0.1})_2Ti_2O_7$ (Ln = Gd, Y, or Yb) exhibits high oxide ion conductivity at high temperatures comparable to YSZ. The $Gd_2(Ti_{1-x}Mo_x)_2O_7$ was studied as anode materials that show high electronic conductivity under reducing atmospheres and stable under 6-day test with 10% H_2S–90% H_2 fuels with improved performance.[5] Moreover, $A_2Ru_2O_7$ (A=Bi, Pb) have been studied as cathode materials but suffer for stability problems.[6]

In this study, we synthesized a series of Cr-doped $Y_2Ti_2O_7$ systems to study the effect of dopants to their electrochemical properties. The results are discussed in light of oxygen vacancies, order and disorder transitions using X-ray analysis, ICP-AES, scanning electron microscope (SEM) and electrochemical analysis in order to check its suitability for Solid Oxide Fuel Cells (SOFC).

Experiments

Synthesis and Characterizations

The starting materials were $Ti[O(CH_2)_3(CH_3)]_4$, $Y(NO_3)_3{\cdot}6H_2O$, $Cr(NO_3)_3{\cdot}9H_2O$ (98.5%, Alfa Aesar), citric acid (99.5%, Aldrich), and ethylene glycol (9.3 g, 99.5% Showa). The Cr-doped $Y_2Ti_2O_7$ solid solution phases were synthesized by sol-gel method.[23] In general, each reaction was carried out with stoichiometric amounts of starting reagents $Y(NO_3)_3{\cdot}6H_2O$, $Cr(NO_3)_3{\cdot}9H_2O$, $Ti[O(CH_2)_3(CH_3)]_4$ were dissolved in the de-ionized water and then added to the solution of citric acid (molar ratio of citric acid to metal ions is 2.5:1). A polymeric gel was formed by addition of the ethylene glycol to the solution (molar ratio of citric acid and ethylene glycol was 1:4) and solvent was evaporated at 150 ºC for 3 h. The obtained polymeric gel was pyrolyzed in an oven for one hour at 350 ºC. The final product was obtained after the calcination at 700 ºC for 5 h. The as-synthesized powder was pressed into pellet in 130 mm in diameter by dry pressing with about 250 mg of powder under a pressure of 4 tons. Those samples were subsequently sintered at 1400 ºC for 5 h to achieve dense bulk materials.

Powder X-ray diffraction (XRD) data were collected at room temperature (RT) using a Bruker D8 Advance diffractometer working in Bragg-Brentano geometry and equipped with a Gobel Mirror and a Vantex detector. Cu Kα radiation was used with a 1^o min^{-1} under 40kV/40mA. The CELREF program was used for cell refinements. Elemental analysis was performed by scanning electron microscope/energy dispersive spectrometer (SEM-EDS, JEOL JSM-4701) and inductively coupled plasma-atomic emission spectrometer (ICP-AES, Jarrell-Ash, ICAP 9000, USA).

The surface composition and oxidation states of each atoms in the as-prepared samples were identified by X-ray photoelectron spectroscopy (XPS) on a KRATOS AXIS Ultra DLD spectrometer equipped with a hemispherical electron analyzer and an

Al anode (Al K = 1486.6 eV) powered at 150 W, a pass energy of 20 eV. The peaks were referenced to the C 1s line at 284.5 eV. Background subtraction using the Shirley method and peak fitting to theoretical Gaussian–Lorentzian functions were performed using an XPS peak program.[7]

Temperature-programmed reduction (TPR) was carried out using a China Chromatography 660 instrument equipped with a TCD detector. A sample of approximately 50 mg was loaded into a quartz tube and sealed with silica wool. The sample was reduced with 5% H_2-Ar flow heated at a rate of 10 ºC·min^{-1} from room temperature to 900 ºC To test the redox stability of $Y_2Ti_{2-x}Cr_xO_7$, these materials were respectively reduced in a cylindrical quartz chamber at 700 ºC and 800 ºC. Temperatures increased at a rate of 10 C/min from room temperature to the desired temperature, and maintained for 5 h under flow of pure H_2. After the treatment, the samples were cooled down to room temperature under the same atmosphere.

Electrochemical analysis

The electrical conductivity of the dense samples (13 mm in diameter and ~1 mm thickness) was evaluated in air and 5% v/v H_2/N_2 with a four-probe dc method from 600 ºC to 900 ºC. Platinum paste (SINETEK CO.) was painted on the surface of pellet, four Pt wires contacts were made, the distance between two neighboring probes were essentially the same. The device was dried at 100 ºC for 1 h to ensure good contact. The electric current between two Pt electrodes was fixed at 50 mA using a Jiehan 5600 current source.

The total (bulk + grain boundary + electrode) ionic conductivities of the prepared $Y_2Ti_{2-x}Cr_xO_7$ samples were measured on sample pellets of approximately 13 mm diameter and 1 mm height. The sample pellets were connected to the silver wire hook via the applied silver electrodes. Ag/Pd paste (SINETEK CO.) was used to ensure good contact between the electrodes and the sample. All measurements were carried out under air, over a temperature range of 600 ºC to 900 ºC in flowing O_2 and 5% v/v H_2/N_2 flow. All measurements were sustained for 30 minutes at each temperature to ensure equilibrium was attained. The data were recorded at 50 ºC intervals, using a Solartron SI 1287 Frequency Response Analyzer over a frequency range from 0.1 Hz to 1 MHz and a voltage of 0.5 V is applied. The EIS data were analyzed using Zview software.

Results and discussion

Characterizations of $Y_2Ti_{2-x}Cr_xO_7$

The phase width of solid solution $Y_2Ti_{2-x}Cr_xO_7$ was studied by PXRD (Figure 1). The results of PXRD analysis indicates that the pure phase of $Y_2Ti_{2-x}Cr_xO_7$ is in a range of x = 0 - 0.8. When x > 0.8 Cr_2O_3 start to formed. The effect of the Cr doping on the crystal unit cell is shown in the Figure 1 insert, which is a function of the cell volume versus molar ratio of Cr. The PXRD patterns of $Y_2Ti_{2-x}Cr_xO_7$ are refined as cubic, space group Pmma with cell parameters within 10.00 - 10.09 Å (JCPDS No.89-2065). The results indicate that the lattice volumes decrease as the amount of doped Cr element increased. According to literature, the Cr ions with oxidation state lower than +4 has a larger ionic radius (Cr^{3+}~ 0.615 Å) than that of Ti^{4+} ion (~ 0.605Å), and a smaller ionic radius was

observed for the oxidation states higher than +4. Hence, the oxidation state of Cr ions in the samples as prepared was expected to be higher than 3+.

Thermal stability of as-synthesized samples was studied by exposing under H_2 atmosphere at high temperature. Based on the results of XRD patterns for samples reduced at 700 ºC and 800 ºC, the products are stable under 100% H_2 flow at 700 ºC for 5 h, and the treatment leads to a decrease of oxidation state as reflecting the expansion of cell dimensions. For reduction under 800 ºC, all samples decomposed and a minor phase Cr_2O_3 was identified. Chemical compositions for these as-prepared powders were determined by ICP-AES and SEM-EDS analysis and the results are listed in Table I. The compositions for all samples are consistent with the stoichiometric ratio from experiments.

Temperature-programmed Reduction

The TPR profiles for $Y_2Ti_{2-x}Cr_xO_7$ are plotted versus the temperature show in Figure 2. As illustrated, there is only one broad peak with the temperature range of 300 - 450 ºC. The reducing temperature shifts slowly to higher temperature and simultaneously increases in intensity with increasing substitution amount of Cr ions, indicative of enhances redox ability due to effect of doped Cr in the host materials. Because of the bond strength of Cr - O is stronger than Ti - O, it becomes difficult to remove the oxygen from the structure when the Ti is modified by Cr atom. Hydrogen consumption rate for the $Y_2Ti_{2-x}Cr_xO_7$ exhibits a gradual increase as x is increased. However, the total H_2 consumptions per mole of Cr show opposite trend, suggesting that the average oxidation states of Cr^{n+} ions is decreased with increased Cr content.

X-ray Photoelectron Spectra

X-ray photoelectron spectroscopy (XPS) was used to understand the oxidation states. The result is shown in Figure 3. For fresh samples, the binding energies for Y3d and Ti2p are in the 156 eV and 463 eV, which are corresponding the oxidation state of Y^{+3} and Ti^{+4}. The Cr2p spectrum splits into two peaks, one at 579 eV is assigned to the binding energy for Cr^{+6} and the other broad peak centering at 576 eV can be indexed to Cr^{+3}. The results suggest that the materials contain mixed-valence states of Cr^{n+} ($3 < n < 6$), signal of Cr^{+4} and Cr^{+5} are involved in two broad peaks centering at Cr^{+3} and Cr^{+6}. In order to minimize the artificial error, the deconvolution of peak is based on Cr^{+6} and Cr^{+3}.

Relative composition of Cr^{+6} and Cr^{+3} ions was performed by fitting the Cr2p core level peaks. The results indicate that the ratio of Cr^{+6}/ Cr^{+3} decreases as a function of Cr content, from 0.185 (x = 0.1) to 0.168 (x = 0.8). These results are consistent with the TPR analyses that show reduced oxidation states of Cr ions with Cr content.[25,26] This trend indicates that the average oxidation state of Cr^{n+} decreases as the Cr content increases. We propose that the increasing rate of Cr^{+6} ion is slower that that of Cr^{3+}. As the concentration of chromium increases, interatomic distance between Cr^{n+} ion become close, and the average oxidation state of Cr is close to +4 in the lattice. The decreased oxidation state as a function of chromium content lead to the reduction of oxygen vacancies, hydrogen consumption and ionic conductivity.

Ionic conductivity

In general, the ionic conductivity of doped samples is higher than that of undoped samples. The trend of conductivity under O_2 atmosphere shows linear behavior from 600 ºC to 900 ºC (Figure 4). The value of ionic conductivity increase with x and maximized at x = 0.2 with log σ = 1 x 10^{-2} S/cm at 700 ºC, and droped gradually when x > 0.2. The calculated Ea (activation energies) are in a range of 0.44-0.82 eV which is lower than previous studies of commercial electrolyte.[8, 9] Under 5% v/v H_2/N_2, the ionic conductivity decreases about half order of magnitude (x = 0.2 with log(σ/S·cm^{-1}) = 1 x 10^{-2} at 700 ºC), indicative of p-type conductor. The trend is similar to ionic conductivity measured under O_2 that presenting a maximum at x = 0.2. The activation energies Ea are in a range of 0.47 - 1.10 eV (Figure 5).

An increase in conductivity in Cr-doped $Y_2Ti_2O_7$ is due to the higher concentration of carriers. When a fraction of Ti^{+4} in $Y_2Ti_2O_7$ is replaced by Cr^{+6} cations, the increase in the positive charge can be compensated by the formation of the oxygen defect (interstitial), and these defects leads to an increased in ionic conductivity. The ionic conductivity maximized at x = 0.2. For samples with x > 0.3, the concentration of defect vacancies decreased so did the ion mobility.[10,11] The drop in ionic conductivity under reducing condition is due to the fact that the oxidation state of Cr is reduced to lower oxidation, hence, decreases the number of interstitial oxygen and drops in ionic conductivity. Ionic conductivity for the $Y_2Ti_{2-x}Cr_xO_7$ oxides, as function of oxygen partial pressure at 700 ºC is shown in figure 6. We observe that as the oxygen partial pressure is increasing, the ionic conductivity is increase as well, following the property of a p-type conductor. The ionic conductivity for $Y_2Ti_{2-x}Cr_xO_7$ (x=0.2) is better that that of YSZ, indicating that $Y_2Ti_{1.8}Cr_{0.2}O_7$ is a potential candidate for electrolyte material in IT-SOFC.

Electrical Conductivity

Arrhenius plots of electrical conductivity were measured in air (oxidation condition) and 5% v/v H_2/N_2 (reducing condition) in the temperature 600 ºC -900 ºC by four-probe method. Figure 7 show the temperature dependence of the conductivity of $Y_2Ti_{2-x}Cr_xO_7$ in air and 5% v/v H_2/N_2 respectively. The increase in conductivity of these samples with the increase in temperature indicates that these materials have a semiconductor property. Under O_2, the electrical conductivity shows similar trend with ionic conductivity which the electrical conductivity increases after initial doping, then decreases with further doping. The conductivities at 700 ºC are maximized at x = 0.2 with log(σ /S·cm^{-1}) T = -0.41 K. Under 5% v/v H_2/N_2, the electrical conductivity is lower than under O_2, indicative of a p-type semiconductor.

The results indicate that the effect of doped chromium ions enhance the electrical conductivity of $Y_2Ti_{2-x}Cr_xO_7$, which may due to the small polaron conduction mechanism.[31] Based on the results from XPS study, the ratio of Cr^{6+} / Cr^{3+} increases with decreasing x. This leads to enhance the electrical conductivity as the concentration of small polarons increase. It then reaches a maximum value at x = 0.2. At higher dopant levels, polarons start to interact with each other and impede mobility and thus, electronic conductivity.

Conclusions

$Y_2Ti_{2-x}Cr_xO_7$ (x=0-0.8) were successively prepared via sol-gel. XPS revealed the presence of Cr^{+3} and Cr^{+6}, and the ratio of Cr^{+6} / Cr^{+3} decreased with the increased Cr content. The presence of Cr^{+6} increased the concentration of carriers that increased the ionic conductivity until the maximum of x = 0.2. The defect starts to interact with each other and reduce carrier's mobility when x > 0.2. The optimized ionic conductivity of $Y_2Ti_{2-x}Cr_xO_7$ is higher than the YSZ and close to GDC in the temperature range of 600-900ºC. The electrical conductivity is also lower than that of GDC. These materials were stable after exposure to 100% H_2 at 700 ºC and unstable at 800 ºC. $Y_2Ti_{2-x}Cr_xO_7$ exhibits high ionic conductivity, low electrical conductivity and stable under reducing environment, which is anticipated to be a potential electrolyte material for IT-SOFCs.

Acknowledgments

This project was supported by MOE ATU program and National Science Council, Taiwan (NSC98-2113-M-009-007-MY3, 98-3114-E-009-006, and 99-3113-P-009-005).

References

1. Huijsmans J. P. P., van Berkel, F. P. F., Christie, G. M. J. Power Sources **71** (1998) 107.
2. Yang L., Wang, S. Z., Blinn, K., Liu, M. F., Liu, Z., Cheng, Z., Liu, M. L. Science **326** (2009) 126.
3. Blundred G. D. B., C. A., Rosseinsky, M. J. Angew. Chem. **43** (2004) 3562.
4. Subramanian M. A., Aravamudan, G., Rao, G. V. S. Prog. Solid State Chem. **15** (1983) 55.
5. Cheng, Z., Liu, M. L. ECS Transactions **1** (2006) 293.
6. Jaiswal A., Wachsman, E. Ionics **15** (2009) 1.
7. Yang D.-Q., Sacher, E. Langmuir **22** (2005) 860.
8. Chen C. C., Nasrallah, M. M., Anderson, H. U. Solid State Ion. **70** (1994) 101.
9. Heiroth S., Lippert, T., Wokaun, A., Dobeli, M., Rupp, J. L. M., Scherrer, B., Gauckler, L. J. J. Eur. Ceram. Soc. **30** (2010) 489.
10. Frayret C. J. Phys. Chem. C **114** (2010) 19062.
11. Burbano M., Norberg, S. T., Hull, S., Eriksson, S. G., Marrocchelli, D., Madden, P. A., Watson, G. W. Chem. Mat. **24** (2012), 222.

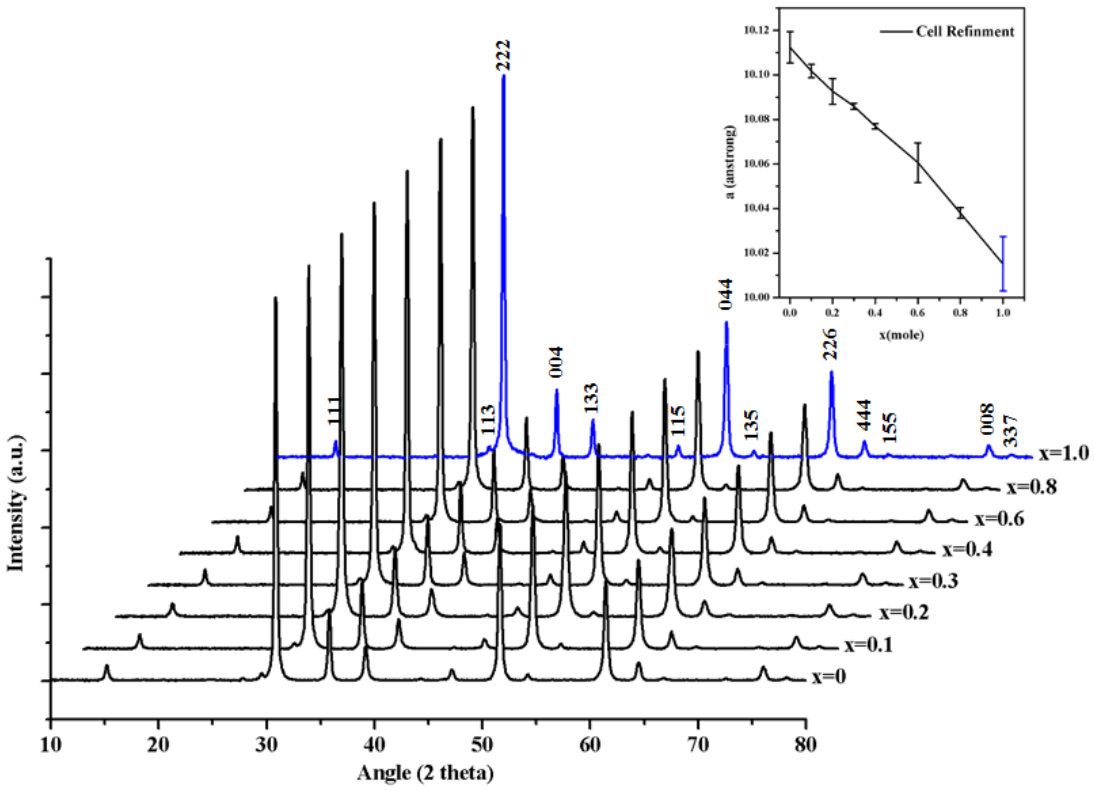

Figure. 1 The XRD patterns of $Y_2Ti_{2-x}Cr_xO_7$ with various Cr doping concentrations (x = 0-1). Inset of lattice parameters in $Y_2Ti_{2-x}Cr_xO_7$ for different Cr-doping contents

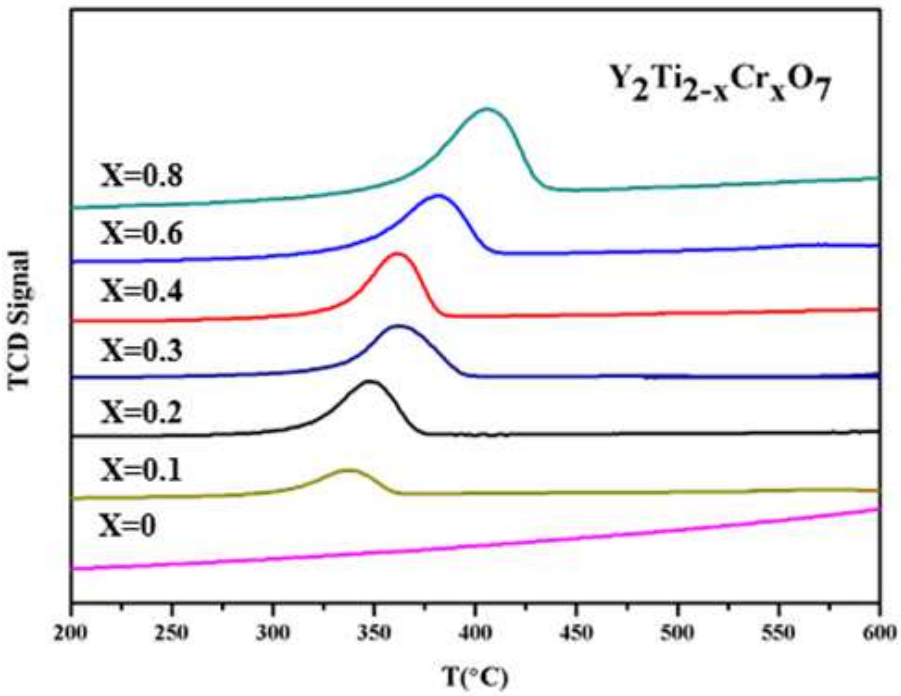

Figure. 2 The TPR profiles of $Y_2Ti_{2-x}Cr_xO_7$ with various Cr doping concentrations (x=0-0.8).

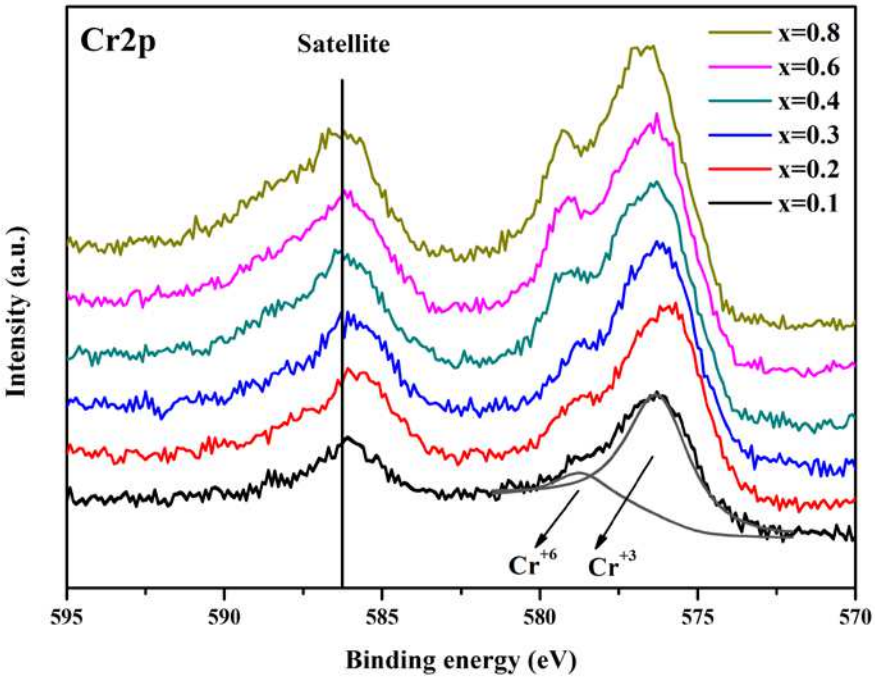

Figure. 3 XPS spectrum of Cr2p for samples of $Y_2Ti_{2-x}Cr_xO_7$. Two peaks were observed; one at 579 eV which could be assigned to Cr^{+6}, and the other broad one can be indexed to Cr^{+3} 576 eV

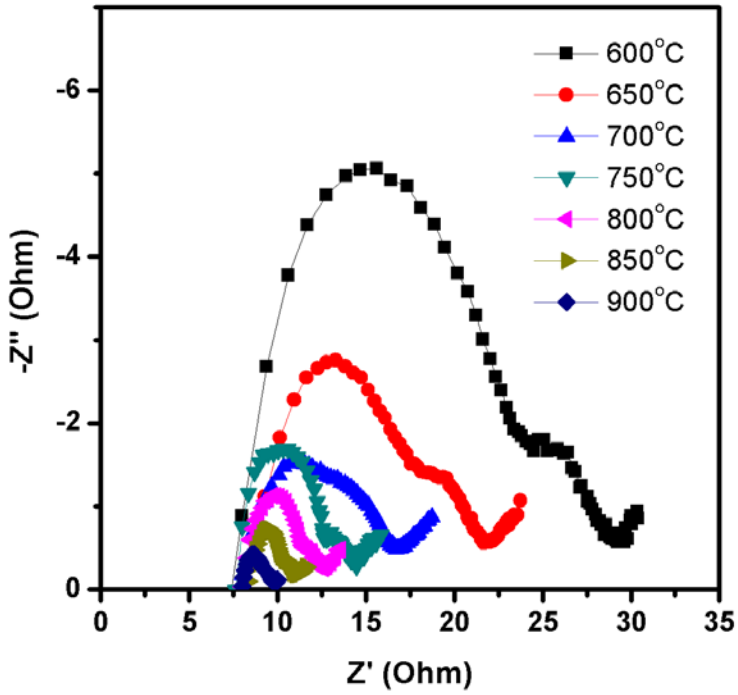

Figure 4. AC-impedance spectrum of $Y_2Ti_{0.9}Cr_{0.1}O_7$ measured from 600 to 900 ºC.

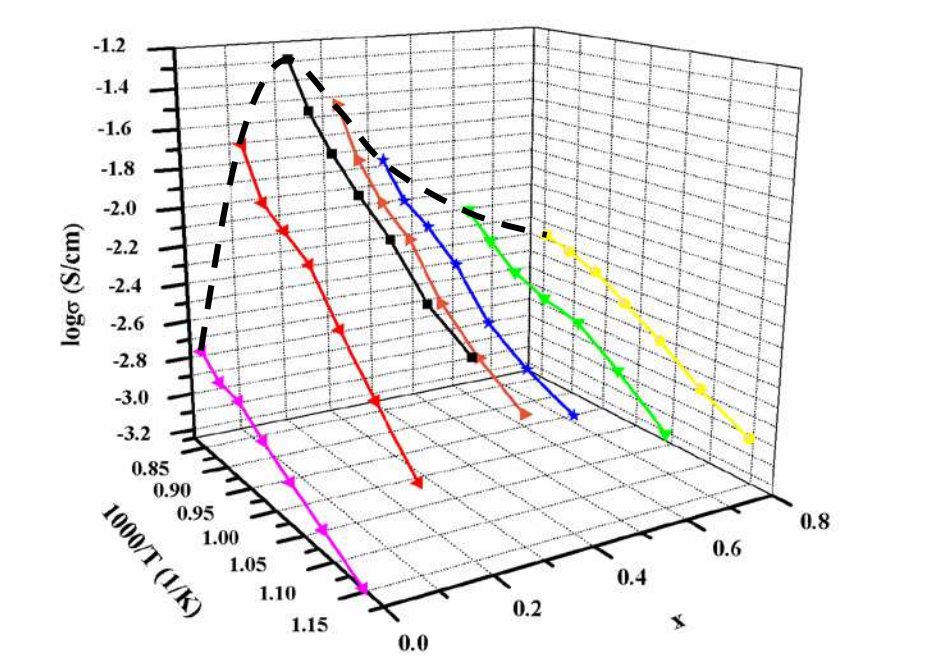

Figure 5. Ionic conductivity of $Y_2Ti_{2-x}Cr_xO_7$ as a function of temperature and Cr doping ratio in O_2 in the temperature of 600 ºC -900 ºC

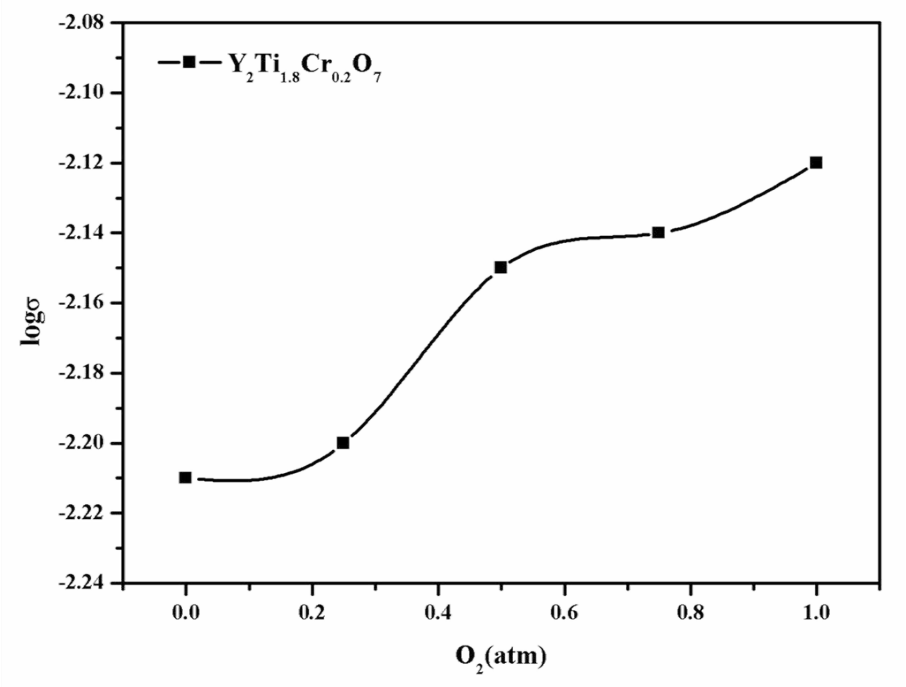

Figure 6. Ionic conductivity for the $Y_2Ti_{2-x}Cr_xO_7$ oxides, as function of oxygen partial pressure at 700 ºC

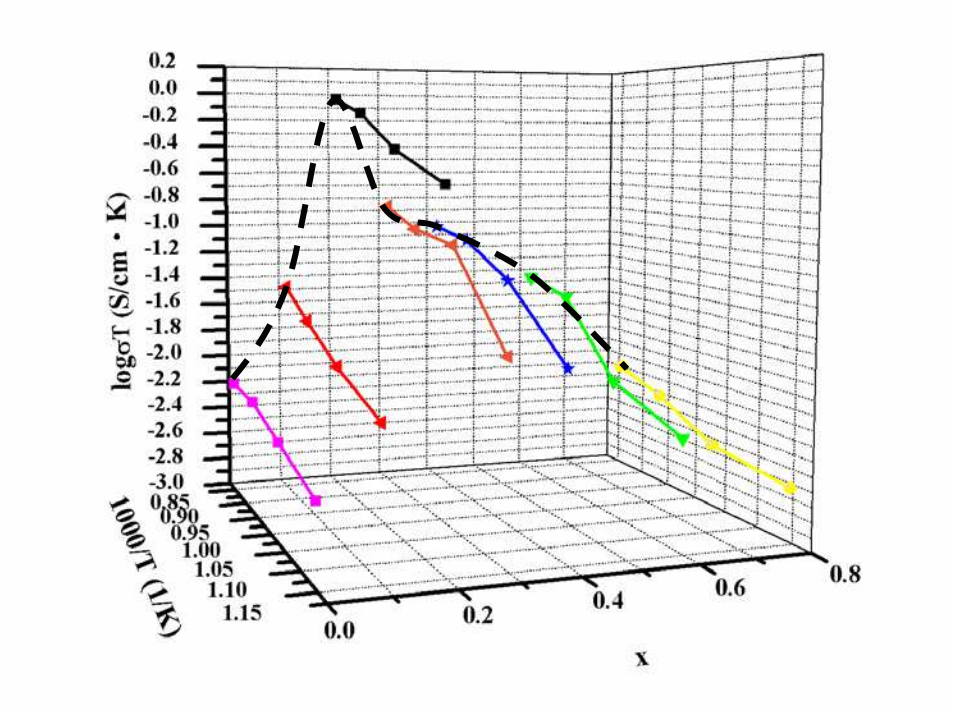

Figure 7. The electrical conductivity of $Y_2Ti_{2-x}Cr_xO_7$ as a function of temperature and Cr doping ratio in air in the temperature of 600 ºC -900 ºC

Table I. Chemical compositions (ICP-AES), (SEM-EDS), H_2 Consumption, The Cr^{+6}/Cr^{+3} values estimated by fitting the Cr2p XPS spectrum

$Y_2Ti_{2-x}Cr_xO_7$	ICP-AES	SEM-EDS	H_2 Consumption (mmole) / sample (g)	H_2 Consumption (mmole) / Cr_{mmole}	Cr^{+6} / Cr^{+3}	Ea (eV) (under O_2)
x=0	NA	NA	—	—	–	-0.44
x=0.1	0.11	0.09	72.7	70.3	0.185	-0.79
x=0.2	0.20	0.18	68.2	70.6	0.181	-0.68
x=0.3	0.34	0.29	72.6	70.2	0.177	-0.54
x=0.4	0.39	0.37	75.0	73.0	0.173	-0.54
x=0.6	0.59	0.60	69.2	64.4	0.170	—
x=0.8	0.76	0.79	67.2	63.1	0.168	—